

Glacial Lake Outburst Floods in the Sagarmatha Region

Authors: Bajracharya, Birendra, Shrestha, Arun Bhakta, and Rajbhandari, Lokap

Source: Mountain Research and Development, 27(4) : 336-344

Published By: International Mountain Society

URL: <https://doi.org/10.1659/mrd.0783>

BioOne Complete (complete.BioOne.org) is a full-text database of 200 subscribed and open-access titles in the biological, ecological, and environmental sciences published by nonprofit societies, associations, museums, institutions, and presses.

Your use of this PDF, the BioOne Complete website, and all posted and associated content indicates your acceptance of BioOne's Terms of Use, available at www.bioone.org/terms-of-use.

Usage of BioOne Complete content is strictly limited to personal, educational, and non - commercial use. Commercial inquiries or rights and permissions requests should be directed to the individual publisher as copyright holder.

BioOne sees sustainable scholarly publishing as an inherently collaborative enterprise connecting authors, nonprofit publishers, academic institutions, research libraries, and research funders in the common goal of maximizing access to critical research.

Birendra Bajracharya, Arun Bhakta Shrestha, and Lokap Rajbhandari

Glacial Lake Outburst Floods in the Sagarmatha Region

Hazard Assessment Using GIS and Hydrodynamic Modeling

336



Glacial lake outburst floods (GLOFs) are common natural hazards in the Himalaya. These floods, usually of large magnitude, can severely affect fragile mountain ecosystems and their limited economic activities. In this

study, GLOF hazard in the Sagarmatha region (national park and buffer zone) was assessed using dam break and hydrodynamic modeling. The available data from the Dig Tsho GLOF of 1985 were used to validate many of the model outputs. The technique was further applied to GLOF hazard assessment of Imja Lake, the largest and potentially most dangerous glacial lake in the region. The peak outflow discharge of an Imja GLOF is estimated at 5463 m³/s. The peak discharge attenuates to about 2000 m³/s at the boundary of the buffer zone at about 45 km from the outburst site. Finally, a GLOF vulnerability rating map was prepared and an assessment of vulnerable settlements was carried out. The study was found to be a cost-effective means of obtaining preliminary information on the extent and impact of possible GLOF events—information that is useful for developing plans for early warning systems and implementing management plans.

Keywords: Mountain hazard; glacial lake outburst flood (GLOF); hydrodynamic modeling; vulnerability; Himalayas; Nepal.

Peer-reviewed: March 2007 **Accepted:** July 2007

Introduction

Climate change and retreating glaciers constitute a major hazard in the Himalayas. The most significant glacial hazards relate to the catastrophic drainage of glacial lakes (Richardson and Reynolds 2000). Such floods caused by the breaking of moraine dams are known as glacial lake outburst floods (GLOFs). The sudden outburst of a glacial lake poses threats of flash floods and debris flow in downstream areas.

Pressures due to increased population and tourism activities in the mountains have caused people to settle in areas which are highly exposed to natural hazards. Trekking routes often lead through unsafe areas, and trails and bridges are situated directly in the floodway. Ives (1986) shows concern over extremely high risks of GLOFs in the Himalayan system, including in the Sagarmatha region, and recommends prior assessment of

GLOFs when planning engineering works. In the context of a new management plan being formulated for the Sagarmatha region (including Sagarmatha National Park and Buffer Zone), which recommends implementing a management zoning system for conservation and promotion of tourism (DNPWC 2005), knowledge about hazardous areas is important for rational planning. Creating awareness among the local people is equally important to discourage development of infrastructure and investment in property in such areas. However, the awareness campaign should not create unnecessary panic, as illustrated by Ives (2004 and 2005) using the example of the Tsho Rolpa case in the Rolwaling Valley.

Keeping in mind that such actions should be based on reliable data and scientific studies, an attempt has been made to assess hazards due to GLOFs from potentially dangerous lakes in the Sagarmatha region, using hydrodynamic models and spatial analysis. Use of hydrodynamic modeling for flood analysis in Nepal is limited to lower mountain catchments (Gautam and Kharbuja 2005), while such exercises are scarcely carried out for high mountain catchments (Cenderelli and Wohl 2001, 2003). The present analysis, however, does not focus on the probability of a lake outburst, but on assessing the extent of resulting floods and identification of the areas susceptible to damage if a GLOF event occurs.

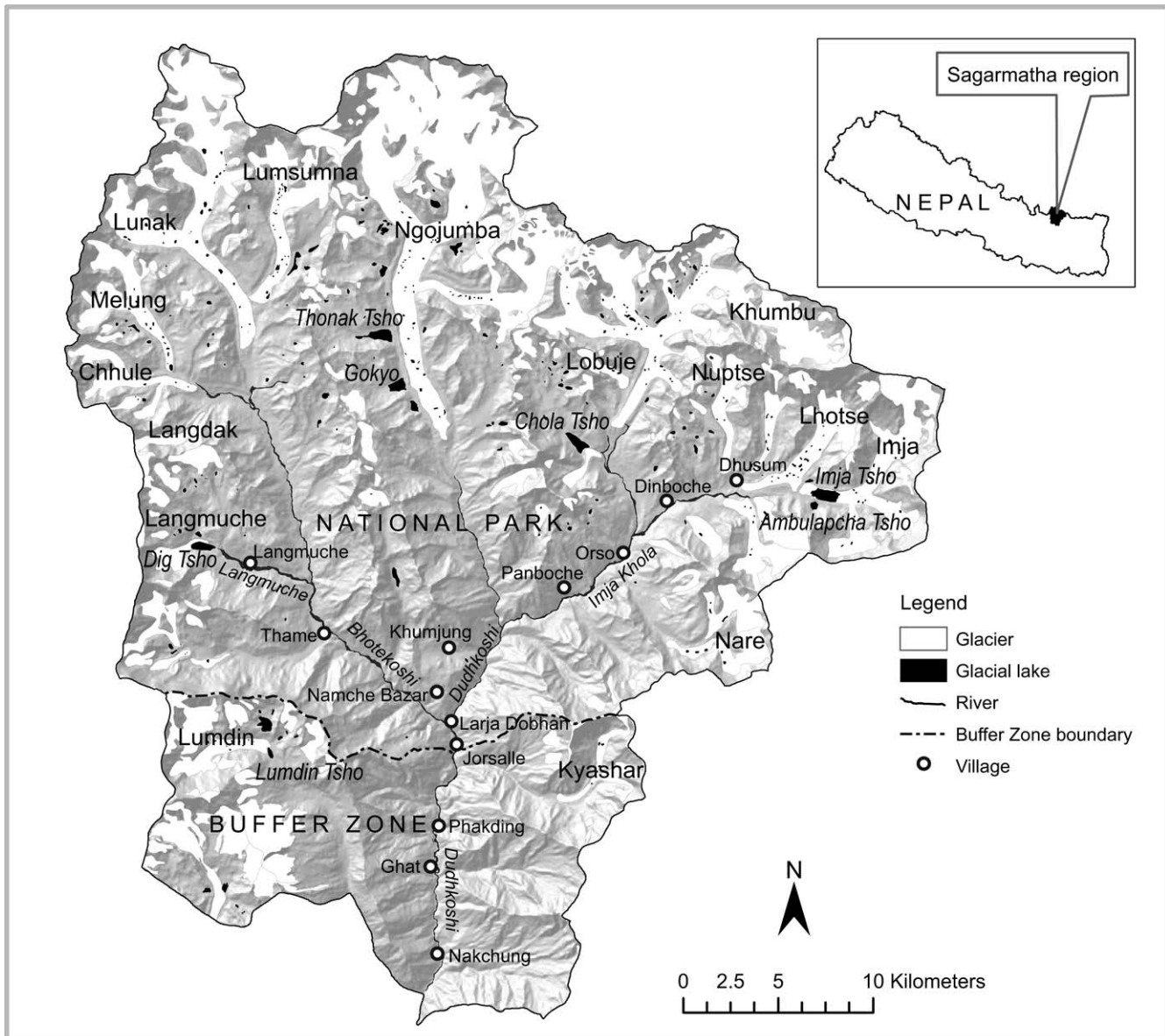
Glaciers and glacial lakes in the Sagarmatha region

The inventory of glaciers and glacial lakes in Nepal prepared by ICIMOD (International Centre for Integrated Mountain Development) has shown that glacial lakes are increasing in number and volume due to thinning and recession of glaciers (Mool et al 2001). It shows that the Sagarmatha region is perhaps one of the most extensively glaciated regions of Nepal (Figure 1). The inventory, based on the reference period from the late 1960s to the early 1970s, recorded 194 glaciers in the region occupying an area of 379.25 km² with a volume of 43.33 km³ of ice. Ngojumba, Khumbu, and Bhote Koshi are the largest glaciers in the region. The number of glacial lakes recorded was 377, occupying a total area of 8.34 km², with a minimum mapped lake size of 424 m². Three lakes—Imja, Dig Tsho, and Lumdin Tsho—were identified as potentially dangerous. Dig Tsho burst out once, on 4 August 1985.

Study area

In the present study, assessment of GLOF hazard was carried out for Imja and Dig Tsho lakes. The assessment of Dig Tsho was done mainly to validate the model outputs, using data from the 1985 GLOF. The assessment was done for the downstream areas of the lakes within the boundaries of the national park and buffer zone.

FIGURE 1 Glaciers and glacial lakes in Sagarmatha region. (Map by authors)



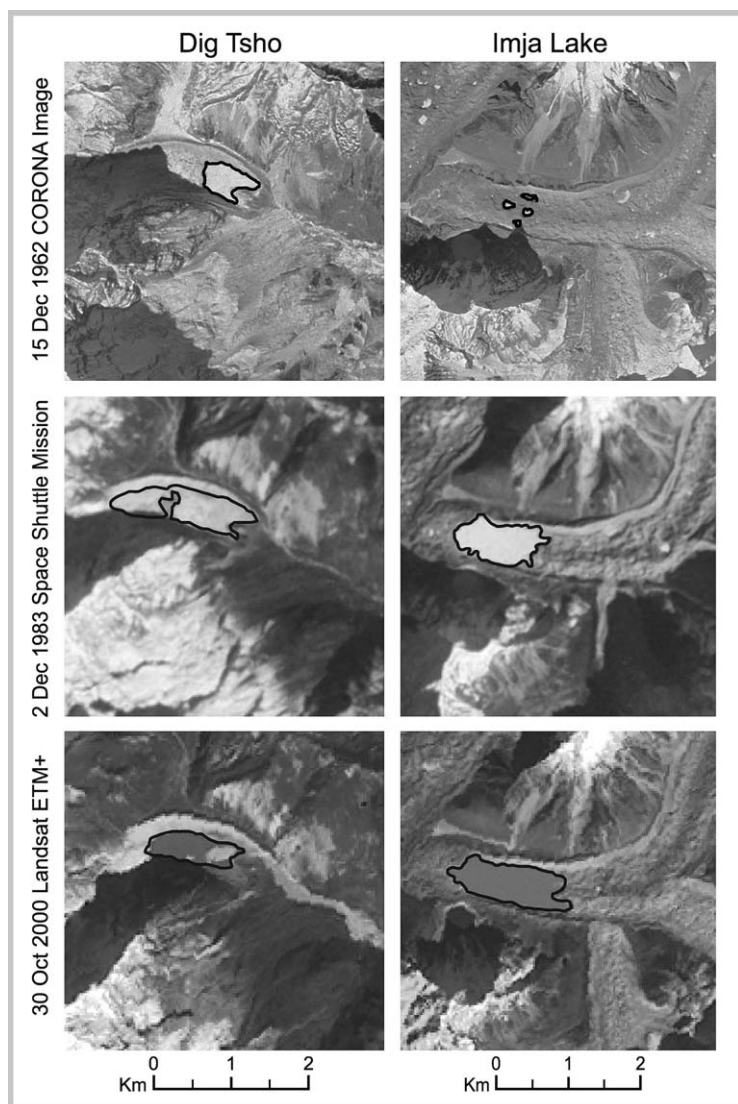
Dig Tsho Lake

Dig Tsho is located at 27°52'25"N and 86°35'37"E, at an elevation of 4365 m, in a sub-basin of the Nangpo-Tsangpo area in Bhote Koshi Valley. The lake is fed by the Langmuche Glacier, which originates at 5400 m at the foot of the northeast face of Tangri Ragi Tau (6940 m) and is extensively nourished by avalanches falling off this rock face. The glacier snout is exposed to heavy solar radiation, which has contributed to the rapid retreat and thinning of the snout in recent decades (Vuichard and Zimmermann 1987).

The development of Dig Tsho was analyzed based on a series of satellite images, some of which are shown in Figure 2. The Corona image of December

1962 shows a lake with a size of 0.2 km². By 1983 this surface had grown to about 0.6 km², which is about 0.1 km² larger than that suggested by Vuichard and Zimmermann (1987) before the outburst. The lake is believed to have been full to its rim just before the outbreak in 1985. The moraine before the breach was 60 m high at its lowest point. The outer slope of the moraine dam is covered with vegetation, while the inner slope is bare and unstable, a characteristic common to moraine dams in contact with a lake. The natural outlet probably ran through the lowest point in the end moraine. The images of 1992 and 2000 suggest the lake might have grown slightly after the outburst and stabilized at an area of around 0.35 km². A

FIGURE 2 Growth of Dig Tsho and Imja lakes. (Maps by authors)



recent field assessment by an ICIMOD team in October 2006 showed a wide outlet, the bottom of which was almost at the level of the valley floor, limiting the possibility of further increase of the lake and future outburst.

Imja Lake

Imja Lake is located at the toe of Imja Glacier, at 27°59'17" N and 86°55'31" E in the easternmost part of the Sagarmatha region. Imja, Lhotse Shar and Ambulapcha are the parent glaciers of Imja Lake. The terminus of Imja Glacier is at about 5010 m. Unlike Dig Tsho, Imja Lake did not exist in the early 1960s: the Corona image of 1962 shows only some small supraglacial ponds (Figure 2). The lake started growing thereafter and attained an area of 0.3 km² in 1975.

Growth was quite rapid, with area in 1983 at 0.56 km², in 1989 at 0.63 km², and in 2000 at 0.77 km².

A study of the expansion process of the lake (Sakai et al 2005) showed that the expanding portion was concentrated near the glacier terminus. According to a field survey in 2001, the area of the lake had attained 0.83 km² (Yamada 2003), which is close to the 0.82 km² measured in the IRS LISS3 image of March 2001. The mean depth of the lake in 2001 was 41 m and the maximum depth was 90 m. The volume of water stored in the lake was estimated at about 35.8 million m³.

The lake is contained by lateral moraines on the north and south, and an end moraine on the west. The 600-m-wide end moraine has an extensive dead ice core that is often exposed, particularly in the vicinity of the outlet. Watanabe et al (1994, 1995) reported rapid melt of the debris-covered ice and significant changes in the outlet position. Enlargement and merger of intermediate ponds in the course of the outlet may cause the lake shoreline to migrate outwards, reducing the width of the dam considerably. This is likely to be a mechanism that could lead to the outburst of the lake.

Methodology

Extraction of geometric and hydraulic information

As it was not possible to survey the detailed geometry in the field, all topographic information required for the study was derived from a digital elevation model (DEM). A DEM with a 5-m grid was derived by interpolating 40-m-interval contour data prepared by the Survey Department of Nepal; the geometric and hydraulic information was extracted using HEC-GeoRAS (USACE 2003). The stream centerline was established from the DEM. The banks were digitized based on topographic maps and IKONOS images with 4-m multispectral resolution and 1-m panchromatic resolution. The reach lengths to be considered for GLOF simulation started at the outlet of moraine dams and terminated at the boundary of the buffer zone. The reach length thus derived was 35.82 km for Dig Tsho and 45.22 km for Imja. River cross-sections were established at 200 m intervals. Altogether, 171 cross sections were delineated for Dig Tsho GLOF simulation and 209 for Imja GLOF simulation. About 1700-m-wide cross-sections were taken, the maximum width HEC-GeoRAS could accept for the DEM resolution used.

Lake information

The bathymetry and the detailed topographic information for the Imja Lake moraine dam were derived from the results of the bathymetric survey of 2001, conducted jointly by a Japanese glaciological expedition in Nepal and the Nepalese Department of Hydrology and Meteorology (Yamada 2003). This information was not

available for Dig Tsho; therefore only the surface area information and maximum depth were used. The analysis was based on average water level and seasonal fluctuations were not taken into consideration.

Dam breach

The geometric data for the Dig Tsho moraine dam were taken from the DEM. As the information regarding geotechnical parameters for both lakes was lacking, these parameters were adapted, similar to the Tsho Rolpa GLOF case study (DHM 1996). NWS-BREACH (NWS 1991) was used to simulate the outburst hydrographs. The model is based on coupling the conservation of mass of reservoir inflow, spillway outflow, and breach outflow with the sediment transport capacity of the unsteady uniform flow along erosion-formed breached channel. It is applicable for both man-made and artificial dams. The growth of breach is dependent on the dam's material properties such as particle size distribution, unit weight, friction angle, and cohesive strength, but does not consider non-homogeneity of the dam material. The outflow hydrograph was obtained through a time-stepping iterative solution not subject to numerical stability or convergence difficulties.

Flood routing

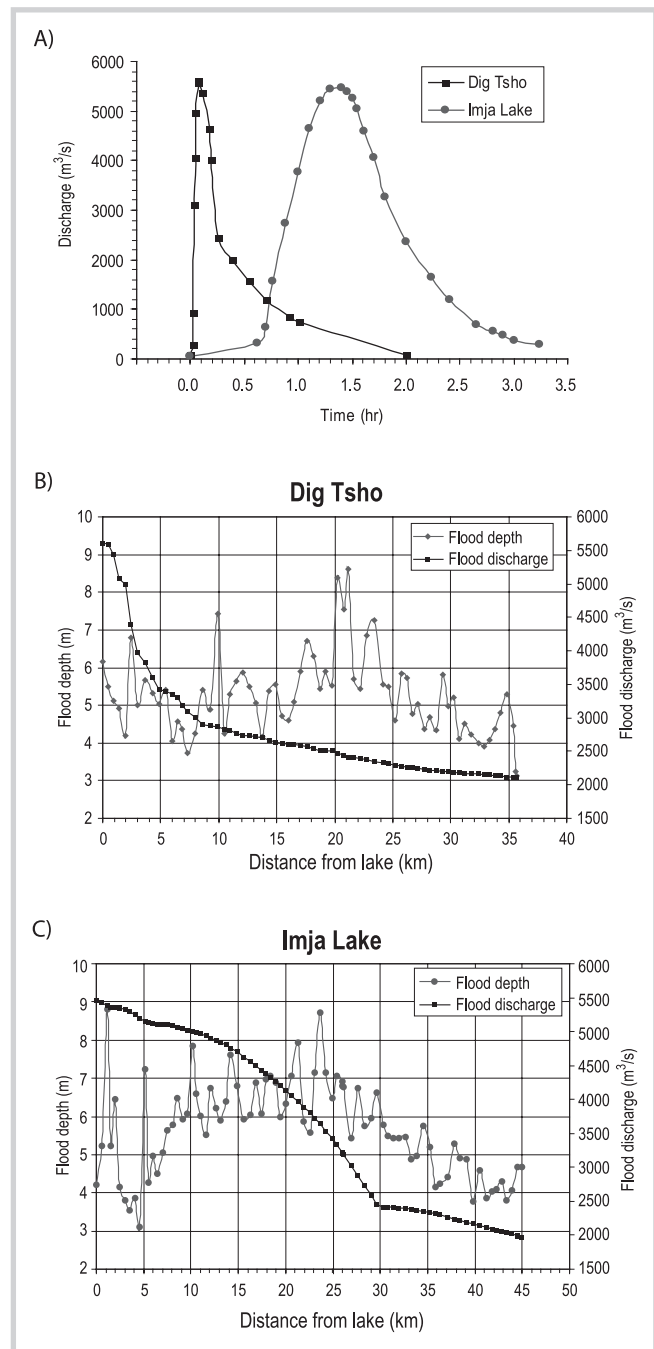
After the GLOF hydrograph was derived from the breach model, the nature of flood propagation in the downstream areas was simulated using NWS-FLDWAV (NWS 1998). It was based on an implicit finite-difference solution of the complete one-dimensional Saint-Venant equations of unsteady flow, coupled with an assortment of internal boundary conditions for simulating unsteady flows controlled by a wide spectrum of hydraulic structures. The model is capable of simulating both Newtonian (water) and non-Newtonian (mud/debris) flows and may freely change with time and location from subcritical to supercritical, or vice versa. Local partial inertial mixed flow technique (NWS 1998) improves the stability of the model when modeling through a mixed-flow situation. In the present study, flow variations were assumed to be constant within individual reaches and between calculation points. The flow hydrograph from NWS-BREACH (Figure 3A) and Manning's n were derived based on IKONOS images provided as inputs for the model.

Flood map

While NWS-FLDWAV simulated the GLOFs successfully, its outputs were limited to numeric results and line graphs. These numeric outputs were fed into the HEC-RAS model set up under steady flow conditions. All the cross-sections included in NWS-FLDWAV were considered as flow change points in HEC-RAS steady flow data, and the peak discharges at these cross-sections were given as

flow input at the respective points. This resulted in relatively smooth highest flood levels (HFLs) along the river reaches. The HFL data for all cross-sections were exported back to HEC-GeoRAS, which has its internal algorithms to generate inundation and flood depth maps.

FIGURES 3A–3C A) Flow hydrographs from NWS-BREACH for Dig Tsho and Imja Lake; B) Peak flow and maximum flood depth due to simulated Dig Tsho GLOF; C) Peak flow and maximum flood depth due to simulated Imja Lake GLOF.



Results and discussion

Dam breach

For this study, only 1 scenario of dam breach was considered. The peak flood discharges of both GLOFs were almost equal, whereas the outflow duration of Imja outburst was considerably longer (Figure 3A), which was probably due to the large width of its moraine dam. The peak outflow of Dig Tsho simulation was significantly larger than those proposed in earlier studies (Vuichard and Zimmermann 1987; Cenderelli and Wohl 2001, 2003). Cenderelli and Wohl (2001, 2003) used a step-backwater model, with the major assumption that the flow was subcritical and approaching supercritical. Discrepancies with the present study could be due to the different methodologies and assumptions made. The simulated peak flood was an estimate on the higher side, but subsequent discussion clarified that the peak flow could not be as low as indicated by Vuichard and Zimmermann (1987).

Flood routing

The peak flow and maximum flood depth along the river reaches are shown in Figures 3B and 3C. Again, there is a sharp contrast between the Dig Tsho and Imja GLOF outflow attenuation along the river. In the case of Dig Tsho, the peak discharge at a distance of 10 km is about $2800 \text{ m}^3/\text{s}$, only about half the peak outflow at the breach site. The peak flow attenuation thereafter is much less, and at the boundary of the Sagarmatha region the peak flow is about $2100 \text{ m}^3/\text{s}$. On the other hand, the attenuation of Imja Lake GLOF is greatly dampened. The peak discharge of $5400 \text{ m}^3/\text{s}$ at the outlet of the lake is considerably sustained through the river reach up to 30 km, following a convex curve which is attributed to the relatively spread outflow hydrograph of Imja outburst.

In the case of the peak flood depth along the rivers, there is quite a lot of scatter over the river reaches, as

higher depth of flooding occurs at narrow river sections. The peak flood depth is greater in the case of Imja GLOF, by about 2 m on average. The divergence in peak flood depth is even greater 16 km before the boundary. After this the flood depths for the 2 GLOFs are of comparable magnitude.

The peak flood depth for Dig Tsho GLOF simulation was compared with the field data collected after the 1985 Dig Tsho GLOF. One such measurement was collected by Maskey (1997), while the other was collected by the Nepal Electricity Authority (NEA 1998). The comparison between the simulation and the NEA observation is presented in Figure 4. There is a reasonable match between simulation and the observed data up to a distance of 18 km. Thereafter, up to 24 km, the observation shows rather high flood depth, up to 13 m. Simulation also suggests maximum flood depth around this reach, although the magnitude is not greater than 8 m. Observation data are virtually non-existent after 24 km. Manning's n was increased by 0.02 over a reach between 10 km and 25 km. A significant increase in HFL occurs between 18 and 24 km, the peak flood depth being comparable to observed data. This shows the sensitivity of the model to the roughness coefficient and the importance of right choice for accurate simulation. It is noteworthy that the comparability of simulated and measured flood depths indicates that the peak flow simulated by the NWS-BREACH model was not exceptionally overestimated as compared to Vuichard and Zimmermann (1987) and Cenderelli and Wohl (2001, 2003).

Flood maps

The spatial distribution of flooding was analyzed by preparing inundation maps for HFL along the river (Figure 5). These maps show the spatial extent as well as depth of flooding along the river reach. The flood arrival time and discharge at different locations from the 2 GLOF simulations are given in Table 1. Although the available data from the past GLOF event at Dig Tsho helped to validate the results of the model output, these results should be viewed with caution, keeping in mind the limitations due to data constraints such as the information derived from the DEM, which is not able to capture all the intricacies of the topography. Also, the model parameters such as geotechnical data and hydraulic information play an important role in the model results. One instance of model sensitivity to Manning's n has been demonstrated in this study. Since the model parameters were either estimated or taken from similar studies, there will certainly be some effects on the accuracy of the results.

GLOF vulnerability assessment

The methodology developed by Reynolds Geo-Sciences (RGS 2003) was adopted with slight modification for vul-

FIGURE 4 Comparison between simulated and observed flooding from Dig Tsho GLOF.

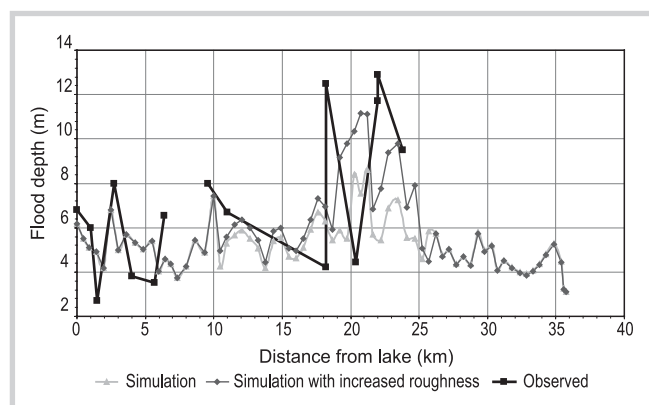
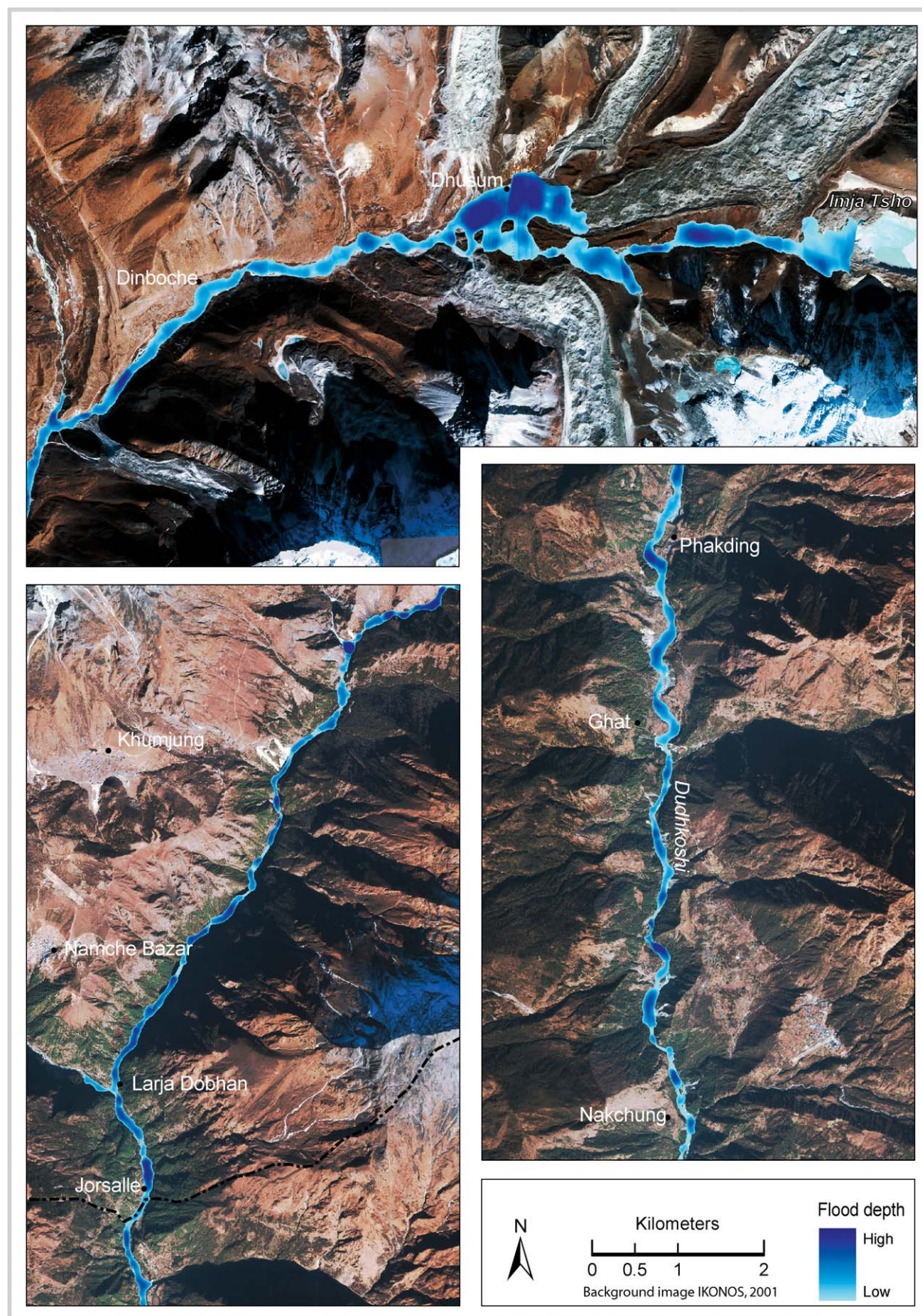


FIGURE 5 Simulated flood map due to Imja Lake GLOF at different reaches. (Maps by authors)



Place	Time (min)	Discharge (m ³ /s)	Flood depth (m)
Dig Tsho GLOF			
Dig Tsho outlet	0.0	5610	6.2
Langmuche	4.80	4986	4.2
Kamthuha	9.00	3592	5.3
Hungmo	13.20	3300	4.6
Thame	21.60	2897	5.4
Larja Dovan (confluence)	30.00	2577	5.5
Nakchung	60.60	2145	5.2
Imja Lake GLOF			
Imja Lake outlet	0.0	5461	4.2
Dhusum (Chukung)	8.8	5242	3.8
Dinboche	13.9	5094	5.8
Orso	18.8	4932	5.5
Panboche	21.3	4800	7.6
Larja Dovan (confluence)	34.8	3223	6.9
Bengkar	38.8	2447	6.6
Ghat	46.4	2355	5.7
Nakchung	55.0	2166	3.8

TABLE 1 Flood arrival time and discharge from Dig Tsho and Imja Lake GLOFs.

TABLE 2 GLOF vulnerability rating scheme (based on RGS 2003).

Vulnerability rating maps	Scoring criteria	Vulnerability Index score	Weighting
Map 1: Compactness	Glacial deposit	1	2
	Cohesive sediment	2	
	Loose sediment	3	
Map 2: Slope map	0–2°	1	1
	2–11°	2	
	> 11°	3	
Map 3: River meandering	Inside bend of a meander	1	1
	Straight	2	
	Outside bend of a meander	3	
Map 4: Land use	Scrub/forest, no human activities	0	3
	Pasture	1	
	Agriculture, commercial forestry	2	
	Infrastructure	2.5	
	Settlement	3	

TABLE 3 Settlements vulnerable to Imja Lake GLOF.

Settlement		Description
#	Name	
1	Dhusum (Chukhung)	Whole village within flood zone.
2	Dinboche	Part of agricultural land and a few houses within flood zone. Almost all agricultural land in northeastern part and half in southern part in highly vulnerable zone.
3	Churo	Agricultural land in highly vulnerable zone.
4	Orso	Agricultural land along riverbank in highly vulnerable zone.
5	Syomare	Agricultural land and some houses in highly vulnerable zone.
6	Panboche	Part of agricultural land along riverbank in highly vulnerable zone.
7	Milingo	Edge of agricultural land along riverbank in highly vulnerable zone.
8	Deboche	Some houses on edge of cliff along riverbank in highly vulnerable zone.
9	Jorsalle	Some houses and agricultural land along riverbank in highly vulnerable zone.
10	Chhumo	Some houses and agricultural land along riverbank in highly vulnerable zone.
11	Bengkar	Some houses, trails, and agricultural land along riverbank in highly vulnerable zone.
12	Ngombuteng	Some houses and agricultural land along riverbank in highly vulnerable zone.
13	Rangding	Houses and agricultural land in flood zone and highly vulnerable zone.
14	Phakding	Agricultural land along riverbank in flood zone and highly vulnerable zone.
15	Sano Gumela	Agricultural land along riverbank in highly vulnerable zone.
16	Chhermading	Some houses and agricultural land along riverbank in highly vulnerable zone.
17	Chhuthawa	Some agricultural land along riverbank in flood zone.
18	Ghat	Some agricultural land and trails along riverbank in highly vulnerable zone.
19	Lhowa	Some agricultural land along riverbank in highly vulnerable zone.
20	Nakchung	Some agricultural land along riverbank in highly vulnerable zone.

nerability assessment and mapping. Inputs into this scheme were topography (slope), geology and geomorphology (compactness), hydrology (river meandering), and land use. A secondary landslide susceptibility map was not used in the present study due to lack of adequate data. Certain factors are considered to be more important than others in determining vulnerability. For example, land use—particularly in settlement areas—is more critical to vulnerability than channel gradient, which tends to have an indirect effect by influencing erodibility. This importance is reflected in a weighting system applied to the vulnerability rating maps (Table 2).

The weighted score for each map was summed within each zone to produce an overall vulnerability score for any location within the area. The range between the minimum and maximum overall vulnerability scores was divided equally into 3 categories, representing low, moderate, and high vulnerability. These rankings were then plotted on the final summary vulnerability rating map.

A buffer of 50 m from the edges of the flood maps was created and the vulnerability zones within these buffer areas were analyzed. A visual assessment of different settlements was made by superimposing the vulnerability map over the 1-m IKONOS panchromatic

images. The list of the settlements in highly vulnerable areas is given in Table 3. Most of the settlements have agricultural land along the river banks with some scattered houses, primarily in highly vulnerable zones. An overlay of the trails on the flood map shows that about 5.8 km of the trails are highly vulnerable. The major segments are located near Dinboche, Orso, Larja Dobhan, and Bengkar, where the trails run through the flood plains. Since there is great variation among the tourists traveling along the trails during different seasons and at different times of the day, assessment of vulnerability for human life is difficult.

Conclusion

This study is an attempt to use a hydrodynamic model coupled with geo-informatics for pre-processing and

post-processing of data to simulate GLOF impact in Himalayan catchments. Although a number of limitations to this study were discussed earlier, the results have shown that studies such as this can be a cost-effective means of obtaining preliminary information on the extent and impact of possible GLOF events in areas like Sagarmatha, where detailed fieldwork is difficult and expensive. The model outputs also provide information on flood arrival time, discharge, and depth, which is important for devising early warning systems.

The vulnerability maps generated through such exercises provide a scientific basis for identifying who is vulnerable and which infrastructure and agricultural land is most likely to be affected. This information can be of great value in developing better options for management plans and their implementation.

ACKNOWLEDGMENTS

This study was carried out as part of an ICIMOD project, "Study on Potential GLOFs and Risk Assessment in the HKH Region," supported by the UNEP (United Nations Environment Programme), Regional Office for Asia and the Pacific. The authors are grateful to Basanta Shrestha and Pradeep Mool for their support and contributions to the study, and to Gauri Shanker Dangol for his assistance in preparing the graphics and maps.

AUTHORS

Birendra Bajracharya, Arun Bhakta Shrestha, and Lokap Rajbhandari International Centre for Integrated Mountain Development (ICIMOD), Khumaltar, Lalitpur, Nepal. bbajracharya@icimod.org (B.B.); abshrestha@icimod.org (A.B.S.); lrajbhandari@icimod.org (L.R.)

REFERENCES

- Cenderelli DA, Wohl EE.** 2001. Peak discharge estimates of glacial lake outburst floods and "normal" climatic floods in Mount Everest region, Nepal. *Geomorphology* 40:57–90.
- Cenderelli DA, Wohl EE.** 2003. Flow hydraulics and geomorphic effects of glacial-lake outburst floods in the Mount Everest region, Nepal. *Earth Surface Processes and Landforms* 28:385–407.
- DHM [Department of Hydrology and Meteorology].** 1996. *Glacier Lake Outburst Flood Study of the Tama Koshi Basin*. Draft Report prepared by BPC Hydroconsult [Butwal Power Company Ltd]. Kathmandu, Nepal: Department of Hydrology and Meteorology.
- DNPWC [Department of National Park and Wildlife Conservation].** 2005. *Sagarmatha National Park and Buffer Zone Management Plan 2006–2011*. Namche, Nepal: Sagarmatha National Park Office.
- Gautam DK, Kharbuja RG.** 2005. Flood hazard mapping of Bagmati River in Kathmandu Valley using geo-informatics tools. *Journal of Hydrology and Meteorology* 3:1–9.
- Ives JD.** 1986. *Glacial Lake Outburst Floods and Risk Engineering in the Himalaya: A Review of the Langmoche Disaster, Khumbu Himal, 4 August 1985*. Occasional Paper 5. Kathmandu, Nepal: ICIMOD [International Centre for Integrated Mountain Development].
- Ives JD.** 2004. *Himalayan Perceptions: Environmental Change and the Well Being of Mountain Peoples*. London, United Kingdom: Routledge.
- Ives JD.** 2005. Global warming—a threat to Mount Everest? *Mountain Research and Development* 25(4):391–394.
- Maskey PR.** 1997. *Glacial Lake Flood Modelling in the Nepalese Himalaya: A Case Study of Digcho Glacier Lake* [MSc thesis]. Enschede, The Netherlands: International Institute for Aerospace Survey and Earth Sciences.
- Mool PK, Bajracharya SR, Joshi SP.** 2001. *Inventory of Glaciers, Glacial Lakes and Glacial Lake Outburst Floods, Nepal*. Kathmandu, Nepal: ICIMOD [International Centre for Integrated Mountain Development].
- NEA [Nepal Electricity Authority].** 1998. Appendix C: Hydrology, hydraulic and sediment studies. In: NEA [Nepal Electricity Authority]. *Dudh Koshi Hydroelectric Project Feasibility Study*. Vol 4 of 8. Kathmandu, Nepal: Nepal Electricity Authority and CIWEC [Canadian International Water and Energy Consultants].
- NWS [National Weather Service].** 1991. *Simplified Dam-break Flood Forecasting Model*. Silver Spring, MD: Hydrologic Research Laboratory, Office of Hydrology, National Weather Service, National Oceanic and Atmospheric Administration.
- NWS [National Weather Service].** 1998. *NWS FLDWAV Model*. Silver Spring, MD: Hydrologic Research Laboratory, Office of Hydrology, National Weather Service, National Oceanic and Atmospheric Administration.
- RGS [Reynolds Geo-Sciences Ltd].** 2003. *Development of Glacial Hazard and Risk Minimization Protocols in Rural Environments: Guidelines for the Management of Glacial Hazards and Risks*. Project R7816. Mold, United Kingdom: Reynolds Geo-Sciences Ltd.
- Richardson SD, Reynolds JM.** 2000. An overview of glacial hazards in the Himalayas. *Quaternary International* 65/66:31–47.
- Sakai A, Fujita K, Yamada T.** 2005. Expansion of the Imja Glacier Lake in the East Nepal Himalayas. In: Mavlyudov BR, editor. *Glacier Caves and Glacial Karst in High Mountains and Polar Regions*. Institute of Geography, Russian Academy of Sciences, pp 74–79.
- USACE [US Army Corps of Engineers].** 2003. *HEC-GeoRAS Version 3.1.1*. Davis, CA: Institute for Water Resources, Hydrologic Engineering Center.
- Vuichard D, Zimmermann M.** 1987. The 1985 catastrophic drainage of a moraine-dammed lake, Khumbu Himal, Nepal: Cause and consequences. *Mountain Research and Development* 7(2):91–110.
- Watanabe T, Ives JD, Hammond JE.** 1994. Rapid growth of a glacial lake in Khumbu Himal, Himalaya: Prospects for a catastrophic flood. *Mountain Research and Development* 14(4):329–340.
- Watanabe T, Kameyama S, Sato T.** 1995. Imja glacier dead-ice melt rates and changes in a supra-glacier lake, 1989–1994, Khumbu Himal, Nepal: Danger of lake drainage. *Mountain Research and Development* 15(4):293–300.
- Yamada T.** 2003. *Research Report of Imja Glacier Lake in Khumbu Region, Nepal Himalaya* [draft]. Kathmandu, Nepal: GEN-GL 2001–2002 glaciological expedition in Nepal and Department of Hydrology and Meteorology.